Computational and Experimental Test of Steric Influence on Agostic Interactions: A Homologous Series for Ir(III)

Alan C. Cooper,[†] Eric Clot,[‡] John C. Huffman,[†] William E. Streib,[†] Feliu Maseras,*[,‡,§] Odile Eisenstein,*[,‡] and Kenneth G. Caulton*[,†]

Contribution from the Department of Chemistry, Indiana University, Bloomington, Indiana 47405-4001, and LSDSMS (UMR 5636) Case Courrier 14, Université de Montpellier 2, 34095 Montpellier Cedex 5, France

Received May 18, 1998

Abstract: Chloride abstraction (using $NaBAr'_4$, $Ar' = 3,5\text{-}(CF_3)_2C_6H_3$) from $Ir(H)_2Cl(P^tBu_2Ph)_2$ gives *cis*,*trans*-$Ir(H)_2(P^tBu_2Ph)_2^+$, which has two agostic interactions with methyl C−H groups on different ^{t}Bu groups. The molecule exists as diastereomers, due to stereochemistry at P. Chloride can be similarly abstracted from ortho-metalated $IrH(\eta^2\text{-}C_6H_4P^tBu_2)Cl(P^tBu_2Ph)$ to give square-pyramidal $IrH(\eta^2\text{-}C_6H_4P^tBu_2)(P^tBu_2Ph)^+$, which has only *one* agostic interaction, involving a ^{t}BuC−H bond; steric constraints on each phosphine leave no more C−H bonds available to donate to the remaining empty Ir(III) orbital. The smaller ligand PCy_2Ph yields only the tris-phosphine complex $Ir(H)_2(PCy_2Ph)_3^+$, and this is shown to have a square-pyramidal structure with one agostic cyclohexyl group and large P_{ax}−Ir−P angles (104−106°). The analogous $Ir(H)_2(P^iPr_2Ph)_3^+$ has similar inter-phosphorus angles, but *no* agostic interaction. Geometrical optimization of $IrH_2L_3^+$ (PCy_2Ph, P^iPr_2Ph) with the hybrid quantum mechanics/molecular mechanics (QM/MM) method (IMOMM) at the IMOMM (B3LYP:MM3) and IMOMM (MP2:MM3) levels permits a more detailed understanding of the influence of steric factors on the occurrence of an agostic bond. The MP2/MM3 method gives the results in closer agreement with experiment. Steric factors place the agostic bond in the vicinity of the metal center but at a distance that is too long to be considered as bonding. The electron-donating ability of the C−H bond and the electron accepting capacity of the metal center, which are introduced only at the QM level, bring the two partners in a bonding situation.

Introduction

The quest for the synthesis of new coordinatively unsaturated transition metal complexes has been driven by the role that these complexes play in many catalytic processes and the useful reactivity that can be exploited for the functionalization of simple organic molecules.[1] It has been proposed that highly unsaturated intermediates in homogeneous catalysis may be stabilized by agostic interactions from ligands on the metal.[2] Shaw et al. first observed that the coordination of bulky tertiary phosphine ligands with the formula P^tBu_2R may stabilize unsaturation in Ir(III) complexes by prohibiting dimerization and solvent coordination.[3] In most studies of unsaturated complexes which include bulky phosphine ligands, the ligands have exhibited a "benign" influence in terms of providing steric protection of empty coordination sites without any direct interaction with the metal beyond metal−phosphorus bonding. However, notable exceptions exist where intramolecular C−H activation (i.e., oxidative addition) of alkyl groups on a phosphine occurs to give metalated-phosphine complexes.[4] Indeed, the metalation of phosphine C−H bonds has been demonstrated to facilitate reductive elimination from Ir(III) complexes.[5] A more subtle influence of bulky phosphine ligands on coordinatively unsaturated metal complexes is found in the interactions of phosphine C−H bonds with the metal center that do not result in a formal oxidative addition of the C−H bond. These interactions, known as agostic bonding,[6a] involve 3-center, 2-electron bonding similar to that observed in main group Lewis acids such as diborane. Agostic bonding has been observed in transition metal complexes for over 30 years but has received more attention in recent years as the number of documented examples have increased greatly.[6b] The bonding of a C−H fragment to a empty metal coordination site is analogous to the binding of dihydrogen. Indeed, a number of dihydrogen

[†] Indiana University.
[‡] Université de Montpellier 2.
[§] Present address: Unitat de Química Física, Edifici C.n., Universitat Autònoma de Barcelona, 08193 Bellatera, Catalonia, Spain.
* Corresponding authors. E-mail: feliu@klingon.uab.es, odile.eisenstein@lsd.univ-montp2.fr, caulton@indiana.edu.

(1) (a) Collman, J. P.; Hegedus, L. S.; Norton, J. R.; Finke, R. G. In *Principles and Applications of Organotransition Metal Chemistry*; University Science: Mill Valley, CA; 1987. (b) Herrmann, W. A.; Cornils, B. *Angew. Chem., Int. Ed. Engl.* **1997**, *36*, 1048.
(2) (a) Margl, P.; Lohrenz, J. C. W.; Ziegler, T.; Blöchl, P. E. *J. Am. Chem. Soc.* **1996**, *118*, 4434. (b) Grubbs, R. H.; Coates, G. W. *Acc. Chem. Res.* **1996**, *29*, 85.
(3) Empsall, H. D.; Hyde, E. M.; Shaw, B. L.; Uttley, M. F. *J. Chem. Soc., Dalton Trans.* **1976**, 2069.
(4) (a) Cooper, A. C.; Huffman, J. C.; Folting, K.; Caulton, K. G. *Organometallics* **1997**, *16*, 505. (b) For an example of phosphite metalation, see: Bedford, R. B.; Castillón, S.; Chaloner, P. A.; Claver, C.; Fernandez, E.; Hitchcock, P. B.; Ruiz, A. *Organometallics* **1996**, *15*, 3990.
(5) (a) Albéniz, A. C.; Schulte, G.; Crabtree, R. H. *Organometallics* **1992**, *11*, 242. (b) Aizenberg, M.; Milstein, D. *Organometallics* **1996**, *15*, 3317. (c) Cooper, A. C.; Huffman, J. C.; Caulton, K. G. *Organometallics* **1997**, *16*, 1974.
(6) (a) Brookhart, M.; Green, M. L. H. *J. Organomet. Chem.* **1983**, *250*, 395. Brookhart, M.; Green, M. L. H.; Wong, L.-L. *Prog. Inorg. Chem.* **1988**, *36*, 1. (b) Crabtree, R. H. *Angew. Chem., Int. Ed. Engl.* **1993**, *32*, 789.
(7) (a) Kubas, G. J.; Ryan, R. R.; Swanson, B. I.; Vergamini, P. J.; Wasserman, H. J. *J. Am. Chem. Soc.* **1984**, *106*, 451. (b) Kubas, G. J. *Acc. Chem. Res.* **1988**, *21*, 120.

10.1021/ja981727e CCC: $18.00
Published on Web 12/16/1998

complexes have been shown to form agostic C−H bonds in the absence of the dihydrogen ligand.[7]

The importance of steric influences in promoting the metalation of phosphine C−H bonds has been revealed in a number of elegant studies by Shaw et al.[8] Since the earliest examples of phosphine metalation,[9] it has been found that the identity of both the metalated alkyl group and pendant alkyl groups on the phosphine ligand play a crucial role in determining whether metalation will occur. Phosphine metalation often results in the formation of highly strained metallacycles due to the small number of members in the ring. A number of examples have been characterized where four-membered rings[10] and even highly strained three-membered rings[11] have been formed via phosphine C−H activation by unsaturated iridium. This steric enhancement of closure of small rings is why $(Ph_2P)_2CMe_2$ favors chelation to a single metal, while $(Ph_2P)_2CH_2$ is more often found bridging two metals.[12] The effect of alkyl substituents on the formation of strained organic ring systems is described by Ingold[13] and has come to be known as the Thorpe−Ingold or "*gem*-dimethyl" effect.[14] A similar effect has been proposed for the pendant alkyl groups of a metalated phosphine ligand. Due to the larger atomic radius of phosphorus vs carbon, it was found that alkyl groups with a large steric impact (i.e., more bulky than methyl) were necessary to promote the formation of phosphine metallacycles. Shaw has appropriately suggested the terminology "*gem-tert*-butyl" effect upon the basis of his extensive studies with P^tBu_2R phosphine ligands.[8c]

While the role of bulky alkyl groups in phosphine metalation is well documented, their possible role in promoting agostic interactions has not been explored extensively. The characterization of agostic interactions can be very difficult due to the weak nature of the interactions. However, solid-state methods (neutron and X-ray crystallography) and solution methods (low-temperature NMR spectroscopy and IR spectroscopy) can characterize the presence of agostic bonds in coordinatively unsaturated metal complexes. These experimental methods, combined with hybrid quantum mechanics/molecular mechanics calculations (QM/MM), have revealed that changes in the steric profile and geometry of phosphine ligands can determine whether agostic interactions will be formed and, in complexes with two empty coordination sites, whether one or two agostic interactions can be formed.[15] The examples of unsaturated Ir(III) complexes, containing agostic interactions, described herein provide an ideal situation to combine experimental results with several "computational experiments", using a hybrid (QM/MM) methodology (IMOMM).[16,17,18] This method has proven to be successful in the quantification of electronic and steric effects in a number of transition metal systems.[17] In the present study, the IMOMM method enables a deeper understanding of the influence of electronic and steric factors on the occurrence of agostic interactions.

Experimental Section

General Procedures. All manipulations were carried out using standard Schlenk and glovebox techniques under argon. Toluene, pentane, THF, and benzene were dried and deoxygenated over sodium or potassium benzophenone and distilled under argon. Fluorobenzene was distilled from P_2O_5 under argon and stored over activated molecular sieves. C_6D_6, d_8-THF, and d_8-toluene were dried over sodium metal and vacuum distilled before use in a glovebox. CD_2Cl_2 and $CDCl_3$ were dried over CaH_2 and vacuum distilled before use in a glovebox. ^1H (referenced to residual solvent impurity), ^{13}C, ^{31}P (referenced to external 85% H_3PO_4), and ^{19}F (referenced to external $CFCl_3$) NMR spectra were collected on Varian Gemini-300 and Inova-400 spectrometers. IR spectra were collected on a Nicolet 510T FT-IR spectrometer. H_2 (Air Products, zero grade), PCy_2Ph (Aldrich), and P^iPr_2Ph (Organometallics, Inc.) were used as purchased. $Na[BAr'_4]$ was prepared according to a literature procedure[19] and dried under dynamic vacuum (1×10^{-3} Torr) at 150 °C until ^1H NMR assay confirmed the complete removal of water from the bulk sample. $[Ir(COE)_2Cl]_2$,[20] $Ir(H)_2Cl(P^tBu_2Ph)_2$,[21] and $IrH(\eta^2\text{-}C_6H_4P^tBu_2)(Cl)(P^tBu_2Ph)$[21] were prepared using literature methods or modification of the literature method.

$[Ir(H)_2(P^tBu_2Ph)_2][BAr'_4]$. Sodium tetrakis[3,5-bis(trifluoromethyl)-phenyl]borate (1.0 g, 1.13 mmol) and $Ir(H)_2Cl(P^tBu_2Ph)_2$ (762 mg, 1.13 mmol) were dissolved in fluorobenzene (50 mL) with stirring. This homogeneous orange solution was stirred for 2 h at room temperature, precipitating a fine white solid during this time. The solution was filtered and concentrated to 3 mL in vacuo. After layering with ca. 5 mL of pentane, the solution was placed in a −20 °C freezer for 1 week. Yellow crystals were separated from the mother liquor and washed with pentane (3×10 mL). Yield: (1.5 g, 87%). ^1H NMR (CD_2Cl_2, 25 °C): 7.83 (br s), 7.73 (m), 7.63 (m), 7.57 (m), 1.36 (vt, $J_{PH} = 7.6$ Hz), −36.51 (br s). ^1H NMR (C_7D_8, 25 °C): 8.30 (s), 8.15 (s), 7.67 (s), 7.55 (s), 7.24 (m), 7.20 (br s), 7.07 (br s), 0.88 (vt, $J_{PH} = 7.2$ Hz), 0.77 (vt, $J_{PH} = 7.6$ Hz), 0.72 (vt, $J_{PH} = 6.0$ Hz), −36.93 (br apparent t), −37.06 (br apparent t). $^{13}C\{^1H\}$ NMR (CD_2Cl_2, 25 °C): 162.51 (m), 136.38 (vt, $J_{PC} = 6.0$ Hz), 135.47 (s), 132.48 (s), 129.62 (m), 129.34 (s), 129.31 (vt, $J_{PC} = 5.0$ Hz), 128.99 (vt, $J_{PC} = 21.5$ Hz), 126.63 (s), 123.92 (s), 121.22 (s), 118.16 (m), 39.52 (vt, $J_{PC} = 12.4$ Hz), 29.69 (vt, $J_{PC} = 9.9$ Hz). $^{31}P\{^1H\}$ NMR (CD_2Cl_2, 25 °C): 60.2 (s). $^{31}P\{^1H\}$ NMR (C_7D_8, 25 °C): 61.7 (s), 61.9 (s). ^{19}F NMR (CD_2Cl_2, 25 °C): −62.3 (s). IR (C_6D_6): 2625, 2593, 2552 cm^{-1}.

$[IrH(\eta^2\text{-}C_6H_4P^tBu_2)(P^tBu_2Ph)][BAr'_4]$. A solution of $IrH(\eta^2\text{-}C_6H_4P^tBu_2)(Cl)(P^tBu_2Ph)$ (0.4 g, 0.60 mmol) dissolved in 5 mL of CH_2Cl_2 was added to a suspension of sodium tetrakis[3,5-bis(trifluoromethyl)-phenyl]borate (0.68 g, 0.60 mmol) in CH_2Cl_2 (10 mL). This red suspension was stirred at room temperature for 30 min, changing color to orange over this time, and filtered. The resulting orange solution was concentrated to dryness in vacuo. The resulting solid was dissolved in fluorobenzene (10 mL) and again concentrated to dryness. The resulting orange solid was suspended in C_6H_6 (2 mL) and heated to 40 °C, causing the solid to form a dense orange oil at the bottom of the flask. This oil (under C_6H_6) was allowed to cool to room temperature and stand overnight, forming a mass of orange crystals. The crystals were separated from the oil and washed with C_6H_6 (3×2 mL). Yield: (0.65 g, 71%). ^1H NMR ($CDCl_3$, 25 °C): 7.69 (m), 7.61 (m), 7.51

(8) (a) Cheney, A. J.; Mann, B. E.; Shaw, B. L.; Slade, R. M. *J. Chem. Soc., Chem. Commun.* **1970**, 1176. (b) Shaw, B. L. *J. Am. Chem. Soc.* **1975**, *97*, 3856. (c) Shaw, B. L. *J. Organomet. Chem.* **1980**, *200*, 307.

(9) Parshall, G. W. *Acc. Chem. Res.* **1970**, *3*, 139 and references therein.

(10) (a) Perego, G.; del Piero, G.; Cesari, M.; Clerici, M. G.; Perrotti, E. *J. Organomet. Chem.* **1973**, *54*, C51. (b) Empsall, H. D.; Heys, P. N.; McDonald, W. S.; Norton, M. C.; Shaw, B. L. *J. Chem. Soc., Dalton Trans.* **1978**, 1119.

(11) (a) Fryzuk, M. D.; Joshi, K.; Chadha, R. K.; Rettig, S. J. *J. Am. Chem. Soc.* **1991**, *113*, 8724. (b) Al-Jibori, S.; Crocker, C.; McDonald, W. S.; Shaw, B. L. *J. Chem. Soc., Dalton Trans.* **1981**, 1572.

(12) Barkley, J.; Ellis, M.; Higgins, S. J.; McCart, M. K. *Organometallics* **1998**, *17*, 1725.

(13) Ingold, C. K. *J. Chem. Soc.* **1921**, *305*, 951.

(14) Eliel, E. L.; Wilen, S. H.; Mander, L. N. *Stereochemistry of Organic Compounds*; Wiley: New York, 1994; p 682.

(15) Ujaque, G.; Cooper, A. C.; Maseras, F.; Eisenstein, O.; Caulton, K. G. *J. Am. Chem. Soc.* **1998**, *120*, 361.

(16) Maseras, F.; Morokuma, K. *J. Comput. Chem.* **1995**, *16*, 1170.

(17) (a) Wakatsuki, Y.; Koga, N.; Werner, H.; Morokuma, K. *J. Am. Chem. Soc.* **1997**, *119*, 360. (b) Ogasawara, M.; Maseras, F.; Gallego-Planas, N.; Kawamura, K.; Ito, K.; Toyota, K.; Streib, W. E.; Komiya, S.; Eisenstein, O.; Caulton, K. G. *Organometallics* **1997**, *16*, 1979. (c) Ujaque, G.; Maseras, F.; Eisenstein, O. *Theor. Chem. Acc.* **1997**, *96*, 146. (d) Maseras, F.; Eisenstein, O. *New J. Chem.* **1998**, *22*, 5.

(18) (a) Svensson, M.; Humbel, S.; Morokuma, K. *J. Chem. Phys.* **1996**, *105*, 3654. (b) Matsubara, T.; Sieber, S.; Morokuma, K. *Int. J. Quantum Chem.* **1996**, *60*, 1101.

(19) Brookhart, M.; Grant, R. G.; Volpe, A. F., Jr. *Organometallics* **1992**, *11*, 3920.

(20) van der Ent, A.; Onderlinden, A. L. *Inorg. Synth.* **1990**, *28*, 90.

(21) Cooper, A. C.; Caulton, K. G. *Inorg. Chim. Acta* **1996**, *251*, 41.

(m), 7.50 (s), 7.21−7.00 (overlapping m), 1.35 (d, J_{PH} = 14.4 Hz), 1.34 (d, J_{PH} = 14.8 Hz), 1.32 (d, J_{PH} = 16.0 Hz), 1.03 (d, J_{PH} = 14.4 Hz), −41.6 (dd, J_{PH} = 12.0 Hz, $J_{P'H}$ = 9.6 Hz). $^{31}P\{^1H\}$ NMR ($CDCl_3$, 25 °C): 39.7 (d, $J_{P'P}$ = 278 Hz), 6.2 (d, $J_{P'P}$ = 278 Hz). ^{19}F NMR ($CDCl_3$, 25 °C): −62.5 (s).

[Ir(H)$_2$(PCy$_2$Ph)$_3$][BAr′$_4$]. To a slurry of [Ir(COE)$_2$Cl]$_2$ (400 mg, 0.50 mmol) in 10 mL of C_6H_6 was added a solution of PCy_2Ph (825 mg, 3.0 mmol) in 5 mL of C_6H_6. Upon addition, the color changed from yellow to orange and the solution became homogeneous. H_2 was bubbled through the solution for 20 min at room temperature. The volatiles were removed from the resulting orange solution in vacuo to yield an orange solid. This solid was dissolved in fluorobenzene (10 mL) and a solution of Na[BAr′$_4$] (885 mg, 1.0 mmol) in 5 mL of fluorobenzene added with stirring. This solution was stirred at room temperature for 1 h and concentrated in vacuo to 5 mL before filtering. The remaining fluorobenzene was removed in vacuo to yield a orange solid. After transferring the solid to a 5-mL flask, toluene (1.5 mL) was added to form a suspension. Upon heating this suspension to 45 °C the solid dissolved to form a dense red oil. The solution was allowed to cool to room temperature and stand overnight, forming a mass of crystals in the dense oil. The solution was decanted, and the crystals were washed with toluene (3 × 2 mL) to yield a dark yellow crystalline solid (1.22 g, 64%). ^1H NMR (d_8-THF, 25 °C): 7.76 (m), 7.55 (s), 7.40−7.07 (m), 2.41 (br s), 1.69 (br s), 1.40−0.85 (m), −26.05 (br s). ^1H NMR (d_8-THF, −110 °C, hydride ligands only): −5.4 (d, J_{PH} = 107 Hz), −44.8 (br s). $^{13}C\{^1H\}$ NMR (d_8-THF, 25 °C): 162.99 (m), 135.77 (s), 133.56 (s), 131.70 (s), 130.66 (m), 130.35 (m), 130.03 (m), 129.75 (s), 129.55 (m), 127.04 (s), 124.34 (s), 121.63 (s), 118.36 (m), 40.05 (br s), 30.58 (s), 30.17 (br s), 27.77 (br s), 27.53 (s), 27.50 (s), 26.96 (s). $^{31}P\{^1H\}$ NMR (d_8-THF, 25 °C): 28.3 (br s). $^{31}P\{^1H\}$ NMR (d_8-THF, −30 °C): 28.9 (br s, 2P), 28.2 (br s, 1P).^{19}F NMR (d_8-THF, 25 °C): −63.4 (s).

[Ir(H)$_2$(P^{i}Pr$_2$Ph)$_3$][BAr′$_4$]. To a slurry of [Ir(COE)$_2$Cl]$_2$ (450 mg, 0.56 mmol) in 15 mL of C_6H_6 was added a solution of P^iPr_2Ph (1.16 mL, 3.36 mmol) in 5 mL of C_6H_6. Upon addition, the color changed from yellow to red and the solution became homogeneous. H_2 was bubbled through the solution for 20 min at room temperature. The volatiles were removed from the resulting orange solution in vacuo to yield an orange solid. This solid was dissolved in fluorobenzene (10 mL) and a solution of Na[BAr′$_4$] (990 mg, 1.12 mmol) in 5 mL of fluorobenzene added with stirring. This solution was stirred at room temperature for 2 h and concentrated in vacuo to 5 mL before filtering. The remaining fluorobenzene was removed in vacuo to yield a dark orange solid. After transferring the solid to a 5-mL flask, toluene (2 mL) was added to form a suspension. Upon heating this suspension to 60 °C the solid dissolved to form a dense red oil. The solution was allowed to cool to room temperature and stand overnight, forming a mass of crystals in the dense oil. The solution was decanted and the crystals washed with toluene (3 × 2 mL) to yield an orange crystalline solid (1.42 g, 76%). ^1H NMR (d_8-THF, 25 °C): 7.80 (m), 7.58 (s), 7.48−7.27 (m), 2.69 (br s), 1.11 (m), 0.92 (m), −25.38 (br s). ^1H NMR (d_8-THF, −110 °C, hydride ligands only): −5.8 (d, J_{PH} = 104 Hz), −43.8 (br s). $^{13}C\{^1H\}$ NMR (d_8-THF, 25 °C): 163.01 (m), 135.77 (s), 133.29 (s), 131.68 (m), 130.37 (m), 130.06 (m), 129.75 (s), 129.40 (m), 127.04 (s), 124.33 (s), 121.63 (s), 118.36 (m), 28.92 (br s), 20.09 (s), 19.18 (s). $^{31}P\{^1H\}$ NMR (d_8-THF, 25 °C): 35.2 (br s). $^{31}P\{^1H\}$ NMR (d_8-THF, −30 °C): 35.2 (br s, 2P), 34.2 (br s, 1P).^{19}F NMR (d_8-THF, 25 °C): −63.9 (s).

Crystallographic Details for [Ir(H)$_2$(P^{t}Bu$_2$Ph)$_2$][BAr′$_4$]. A crystal of suitable size was obtained by cleaving a large piece of the sample in a nitrogen atmosphere glovebag. The crystal was mounted using silicone grease, and it was then transferred to a goniostat where it was cooled to −167 °C for characterization and data collection (Table 1). A preliminary search for peaks followed by analysis using programs DIRAX and TRACER revealed a triclinic cell. Following intensity data collection a correction for drift in the data was made, based on four standards (0 0 6, −7 0 0, 0−5 0, −2−10 2) measured every 400 data. An analytical correction was also made for absorption. The asymmetric unit contains three cations, three anions, and one molecule of fluorobenzene. The cations, two of the anions, and the solvent molecule were reasonably well ordered, and hydrogens were included for them in fixed calculated positions with thermal parameters fixed at one plus the isotropic thermal parameter of the parent carbon atoms. The third anion was badly disordered and was modeled as 98 atoms, many at partial occupancy. The occupancies were refined, scaled to give a total occupancy of 57 atoms that should have been present, and then fixed. No attempt was made to include hydrogens on the disordered anion. In the final cycles of refinement, isotropic thermal parameters were varied for one atom in the second anion, C(180) whose anisotropic thermal parameters did not refine properly, and for all atoms in the disordered anion. The largest peak in the final difference map was 1.5 e/Å^3 near the disordered anion, and the deepest hole was −1.6 e/Å^3. Two anticipated hydride ligands on each of the iridium atoms were not observed and were not included in the refinement.

Table 1. Crystallographic Data for [Ir(H)$_2$(P^{t}Bu$_2$Ph)$_2$][BAr′$_4$]

a = 20.023(4) Å	fw[a] = 4602.33
b = 28.492(6) Å	space group: $P\bar{1}$
c = 19.579(4) Å	T = −167 °C
α = 109.47(1)	λ = 0.71069 Å[b]
β = 89.89(1)	ρ_{calcd} = 1.562 g cm^{-1}
γ = 110.40(1)	μ = 22.082 cm^{-1}
V = 9788.58 Å^3	$R(F_o)$[c] = 0.0660
Z = 2	$R_w(F_o)$[d] = 0.0595

[a] Formula $C_{180}H_{180}B_3F_{72}P_6Ir_3$; C_6H_5F. [b] Graphite monochromator. [c] $R = \sum||F_o| - |F_c||/\sum|F_o|$. [d] $R_w = [\sum w(|F_o| - |F_c|)^2/\sum w|F_o|^2]^{1/2}$, where $w = 1/\sigma^2(|F_o|)$.

Table 2. Crystallographic Data for [IrH(η^2-C$_6$H$_4$P^{t}Bu$_2$)(P^{t}Bu$_2$Ph)][BAr′$_4$]

a = 12.798(1) Å	fw[a] = 1617.23
b = 23.148(2) Å	space group: $P\bar{1}$
c = 12.220(1) Å	T = −170 °C
α = 92.91(1)	λ = 0.71069 Å[b]
β = 92.99(1)	ρ_{calcd} = 1.543 g cm^{-1}
γ = 74.50(1)	μ = 20.566 cm^{-1}
V = 3481.46 Å^3	$R(F_o)$[c] = 0.068
Z = 2	$R_w(F_o)$[d] = 0.055

[a] Formula $C_{69}H_{67}BF_{24}IrP_2$. [b] Graphite monochromator. [c] $R = \sum||F_o| - |F_c||/\sum|F_o|$. [d] $R_w = [\sum w(|F_o| - |F_c|)^2/\sum w|F_o|^2]^{1/2}$, where $w = 1/\sigma^2(|F_o|)$.

Crystallographic Details for [IrH(η^2-C$_6$H$_4$P^{t}Bu$_2$)(P^{t}Bu$_2$Ph)][BAr′$_4$]. An orange crystal was cleaved to form a nearly equidimensional trigonal prism, affixed to the end of a glass fiber using silicon grease, and cooled to −170 °C for characterization and data collection (Table 2). A systematic search of a limited hemisphere of reciprocal space located 86 reflections which were used to determine that the crystal possessed no symmetry or systematic absences, indicating a triclinic space group. Subsequent solution and refinement confirmed the centrosymmetric choice, $P\bar{1}$. Data were corrected for Lorentz and polarization effects, equivalent reflections, and averaged after an analytical absorption correction (transmission factors 0.41−0.60). The structure was solved using direct methods (MULTAN78) and Fourier techniques. Hydrogen atoms were generally visible in a difference Fourier phased on the non-hydrogen atoms but were placed in idealized fixed positions for the final cycles of refinement. The data were not of sufficient quality to locate the hydride ligand. A final difference Fourier was featureless. There was one peak of 2.45 e/Å^3 at the metal site, and several peaks of up to 2.0 e/Å^3 in the vicinity of the fluorine atoms of the anion.

Crystallographic Details for [Ir(H)$_2$(PCy$_2$Ph)$_3$][BAr′$_4$]. A crystal of suitable size was mounted in a nitrogen atmosphere glovebag using silicone grease. It was then transferred to a goniostat where it was cooled to −168 °C for characterization and data collection (Table 3). A preliminary search for peaks and then analysis using programs DIRAX and TRACER revealed a triclinic cell. Following intensity data collection and an analytical correction for absorption (transmission factors 0.65−0.86), the structure was solved using a combination of direct methods (MULTAN78) and Fourier techniques. The positions of the Ir and 22 other non-hydrogen atoms were obtained from an initial E-map. The positions of the other non-hydrogen atoms were obtained from iterations of a least-squares refinement followed by a difference

Table 3. Crystallographic Data for $[Ir(H)_2(PCy_2Ph)_3][BAr'_4]$

$a = 17.627(3)$ Å	fw = 1919.68
$b = 18.678(3)$ Å	space group: $P\bar{1}$
$c = 13.772(2)$ Å	$T = -168$ °C
$\alpha = 91.13(1)$	$\lambda = 0.71069$ Å[a]
$\beta = 105.65(1)$	$\rho_{calcd} = 1.483$ g cm^{-1}
$\gamma = 99.59(1)$	$\mu = 17.112$ cm^{-1}
$V = 4295.09$ Å^3	$R(F_o)$[b] = 0.042
$Z = 2$	$R_w(F_o)$[c] = 0.041

[a] Graphite monochromator. [b] $R = \sum|F_o| - |F_c|/\sum|F_o|$. [c] $R_w = [\sum w(|F_o| - |F_c|)^2/\sum w|F_o|^2]^{1/2}$, where $w = 1/\sigma^2(|F_o|)$.

Table 4. Crystallographic Data for $[Ir(H)_2(P^iPr_2Ph)_3][BAr'_4]$

formula = $C_{68}H_{71}BF_{24}IrP_3$	space group = $P2_12_12_1$
$a = 17.174(4)$ Å	$T = -170$ °C
$b = 24.980(6)$ Å	$\lambda = 0.71069$ Å[a]
$c = 16.466(3)$ Å	$\rho_{calcd} = 1.542$ g cm^{-3}
$V = 7064.02$ Å^3	$\mu = 20.495$ cm^{-1}
$Z = 4$	$R(F_o)$[b] = 0.0886
fw = 1640.22	$R_w(F_o)$[c] = 0.0592

[a] Graphite monochromator. [b] $R = \sum|F_o| - |F_c|/\sum|F_o|$. [c] $R_w = [\sum w(|F_o| - |F_c|)^2/\sum w|F_o|^2]^{1/2}$, where $w = 1/\sigma^2(|F_o|)$.

Fourier calculation. The asymmetric unit contains one-half molecule of benzene solvent, the center of the benzene molecule being at a crystallographic center of symmetry. Hydrogens bonded to carbons were included in fixed calculated positions with thermal parameters fixed at one plus the isotropic thermal parameter of the parent carbon atom. The hydride ligands could not be identified from the most significant peaks in the final difference Fourier, and none were included in any of the calculations. In the final cycles of refinement, all of the non-hydrogen atoms were varied with anisotropic thermal parameters. The largest peak in the final difference map was 1.7 e/A^3 at the Ir position, and the deepest hole was -0.9 e/A^3.

Crystallographic Details for $[Ir(H)_2(P^iPr_2Ph)_3][BAr'_4]$. A suitable fragment of a larger crystal was mounted on a glass fiber in a nitrogen atmosphere glovebag using silicone grease. It was then transferred to a goniostat where it was cooled to -170 °C for characterization and data collection (Table 4). A systematic search of a limited hemisphere of reciprocal space was used to determine that the crystal possessed orthorhombic symmetry and systematic absences indicating the unique space group $P2_12_12_1$. The structure was solved with absorption corrected data (transmission factors 0.70 to 0.73) using a combination of direct methods (SHELXTL-PC) and Fourier techniques. Hydrogen atoms were visible in a difference Fourier phased on the non-hydrogen atoms and were included as isotropic contributors in the final cycles of refinement. Some difficulty was encountered in modeling disorder in the CF_3 groups of the anion. Several attempts were made to locate the hydride ligands, with no success. A final difference Fourier was featureless, the largest peak being 1.23 e/A^3, located adjacent to the Ir position.

Computational Details. Pure quantum mechanics calculations on the model systems $Ir(H)_2[P(Et)H_2]_2^+$, $Ir(H)_2[P(Et)H(CHCH_2)]_2^+$, $Ir(H)_2(PH_3)_3^+$, and $Ir(H)_2(P(Et)H_2)_3^+$ are carried out with Gaussian 94.[22] Quasirelativistic effective core potentials replace the 60-electron core of the Ir atom[23] and the 10-electron core of the P atoms.[24] The basis set was valence double-ζ for all atoms,[24,25] with the addition of a polarization d shell on phosphorus atoms.[26] A larger basis set including polarization shells on carbon and hydrogen atoms[27] involved in the agostic interaction was discarded because preliminary calculations showed that it brought only very minor differences.

Hybrid IMOMM (integrated molecular orbital/molecular mechanics) calculations were performed with a program built from modified versions of two standard programs: Gaussian 92/DFT[28] for the quantum mechanics (QM) part and MM3(92)[29] for the molecular mechanics (MM) part. A number of different partitions of the molecules in QM and MM regions were used, and they will be detailed as they are presented. The computational level for the QM part was always that described in the previous paragraph. For the MM part, the MM3(92) force field was used.[30]Van der Waals parameters for the iridium atom are taken from the UFF force field,[31] and torsional contributions involving dihedral angles with the metal atom in terminal position are set to zero. All geometrical parameters are optimized without symmetry restrictions except the bond distances between the QM and MM regions of the molecules. The frozen values are 1.420 Å (P−H) and 1.112 Å (C−H) in the QM part and 1.843 Å (P−Csp^3), 1.828 Å (P−Csp^2), 1.5247 Å (C−C) in the MM part. The starting point of all geometry optimizations was the X-ray structure coordinates of the cationic iridium complex.

Results and Discussion

Synthesis and Characterization of $[Ir(H)_2(P^tBu_2Ph)_2][BAr'_4]$. Abstraction of the X ligand from coordinatively unsaturated $Ir(H)_2(X)(P^tBu_2Ph)_2$ (X = Cl, F, OSO_2CF_3) by $Na[BAr'_4]$ (Ar′ = 3,5-bis(trifluoromethyl)phenyl) in fluorobenzene yields the solvent-ligand-free cationic iridium(III) complex $[Ir(H)_2(P^tBu_2Ph)_2][BAr'_4]$ in nearly quantitative yield. An important conclusion from this result is the potent Lewis acidity of sodium in $Na[BAr'_4]$, for its ability to abstract the X ligand even when there is multiple metal−ligand bond character,[32] and when a 14 e$^-$ species is produced. Crystallization occurs from slow diffusion of pentane into a concentrated fluorobenzene solution at -20 °C. This yellow air-sensitive complex is highly soluble in THF, CH_2Cl_2, and acetone and demonstrates moderate solubility in nonpolar arene solvents. The $^{31}P\{^1H\}$ NMR in d_8-toluene shows two singlets, separated by 0.2 ppm, in the temperature range +75 to -40 °C. Agostic bonding from C−H bonds of both phosphines in noncoordinating toluene makes the phosphorus atoms chiral and, therefore, makes possible the observation of diastereomers in the NMR spectra. However, the observation of singlets for both diastereomers indicates that the agostic bonding is fluxional, with a rapid (on the NMR time scale) exchange of agostic bonding to both coordination sites by each phosphine (Figure 1). The ^1H NMR spectrum (25 °C) in d_8-toluene displays multiple signals for the ^{t}Bu protons (with virtual triplet splitting and shifted upfield by 0.5−0.7 ppm in comparison to the ^{t}Bu resonance in CD_2Cl_2), indicating that the phosphines have inequivalent ^{t}Bu groups. This is attributed to agostic bonding, which causes the inequivalence of agostic ^{t}Bu vs pendant ^{t}Bu groups. In addition, there are two resolved signals in the upfield region of the ^1H NMR spectrum for the hydride resonances of two diastereomers. The variable-temperature ^1H NMR spectra in d_8-toluene reveal two dynamic processes

(22) Frisch, M. J.; Trucks, G. W.; Schlegel, H. B.; Gill, P. M. W.; Johnson, B. G.; Robb, M. A.; Cheeseman, J. R.; Keith, T.; Peterson, G. A.; Montgomery, J. A.; Raghavachari, K.; Al-Laham, M. A.; Zakrzewski, V. G.; Ortiz, J. V.; Foresman, J. B.; Cioslowski, J.; Stefanov, B. B.; Nanayakkara, A.; Challacombe, M.; Peng, C. Y.; Ayala, P. Y.; Chen, W.; Wong, M. W.; Andres, J. L.; Replogle, E. S.; Gomperts, R.; Martin, R. L.; Fox, D. J.; Binkley, J. S.; Defrees, D. J.; Baker, J.; Stewart, J. P.; Head-Gordon, M.; Gonzalez, C.; Pople, J. A. *Gaussian 94*: Revision, D. I.; Gaussian, Inc.: Pittsburgh, PA, 1995.

(23) Hay, P. J.; Wadt, W. R. *J. Chem. Phys.* **1985**, *82*, 299.

(24) Wadt, W. R. Hay, P. J.; *J. Chem. Phys.* **1985**, *82*, 284.

(25) Hehre, W. J.; Ditchfield, R.; Pople, J. A. *J. Chem. Phys.* **1972**, *56*, 2257.

(26) Francl, M. M.; Pietro, W. J.; Hehre, W. J.; Binkley, J. S.; Gordon, M. S.; DeFrees, D. J.; Pople, J. A. *J. Chem. Phys.* **1982**, *77*, 3654.

(27) Hariharan, P. C.; Pople, J. A. *Theor. Chim. Acta* **1973**, *28*, 213.

(28) Frisch, M. J.; Trucks, G. W.; Schlegel, H. B.; Gill, P. M. W.; Johnson, B. G.; Wong, M. W.; Foresman, J. B.; Robb, M. A.; Head-Gordon, M.; Replogle, E. S.; Gomperts, R.; Andres, J. L.; Raghavachari, K.; Binkley, J. S.; Gonzalez, C.; Martin, R. L.; Fox, D. J.; Defrees, D. J.; Baker, J.; Stewart, J. P.; Pople, J. A. *Gaussian 92/DFT*; Gaussian, Inc.: Pittsburgh, PA, 1993.

(29) Allinger, N. L. *MM3(92)*; QCPE: Indiana University, 1992.

(30) (a) Allinger, N. L.; Yuh, Y. H.; Lii, J. R. *J. Am. Chem. Soc.* **1989**, *111*, 8551. (b) Lii, J. H.; Allinger, N. L. *J. Am. Chem. Soc.* **1989**, *111*, 8566. (c) Lii, J. H.; Allinger, N. L. *J. Am. Chem. Soc.* **1989**, *111*, 8576.

(31) Rappé, A. K.; Casewit, C. J.; Colwell, K. S.; Goddard, W. A., III; Skiff, W. M. *J. Am. Chem. Soc.* **1992**, *114*, 10024.

(32) Caulton, K. G. *New. J. Chem.* **1994**, *18*, 25 and references therein.

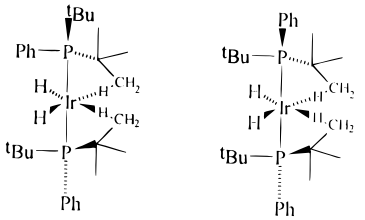

Figure 1. Two diastereomers of doubly agostic $Ir(H)_2(P^tBu_2Ph)_2^+$.

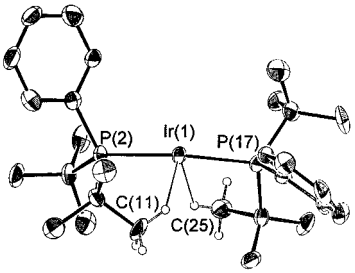

Figure 2. ORTEP drawing of cation 1 of $Ir(H)_2(P^tBu_2Ph)_2^+$, showing selected atom labeling. Only the hydrogens of the agostic methyl groups (placed in idealized positions) are shown.

involving ^{t}Bu protons. Coalescence of pendant and agostic ^{t}Bu groups is only evident at +75 °C. There is also an observed broadening of the agostic ^{t}Bu resonances below −20 °C, attributed to decoalescence of the methyl groups within an agostic ^{t}Bu. Due to the complexity of the ^{1}H NMR spectra resulting from these several dynamic processes, a technique with a faster time scale was necessary for spectroscopic characterization of agostic interactions in solution. The IR spectrum of $[Ir(H)_2(P^tBu_2Ph)_2][BAr'_4]$ in C_6D_6 displays three bands of medium intensity at 2625, 2593, and 2552 cm^{-1}. These are assigned to the agostic C−H stretches of the two diastereomers (Figure 1).[33]

The X-ray structure of $[Ir(H)_2(P^tBu_2Ph)_2][BAr'_4]$ shows that there are three independent $[Ir(H)_2(P^tBu_2Ph)_2]^+$, three noncoordinating[34] $[BAr'_4]^-$, and one (noninteracting) fluorobenzene per asymmetric unit. The fortuitous crystallization of three independent molecules in the unit cell allows for six separate observations of the agostic interactions in three different positions within the crystal lattice, allowing for the averaging of crystal packing effects on bond lengths and angles.[35] Two of the cations (Figure 2) are very similar, with only minor conformational differences within the phosphine ligands, while the third cation (Figure 3) shows opposite chirality at one phosphine relative to the first two cations. In all three cations, there are no close Ir/C(phenyl) contacts (<3.48 Å), but there are two separate agostic interactions from *tert*-butyl C−H bonds to the unsaturated iridium center.[36]

The metal hydrides and the agostic H were not located by X-ray diffraction. The six independently measured agostic interactions are characterized by Ir−C distances of 2.81−2.94 Å. These Ir−C distances are longer than those reported for other agostic interactions among crystallographically characterized Ir(III) complexes,[5a,37] but within the range of reported agostic

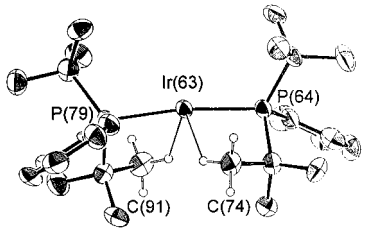

Figure 3. ORTEP drawing of cation 3 of $Ir(H)_2(P^tBu_2Ph)_2^+$, showing selected atom labeling. Only the hydrogens of the agostic methyl groups (placed in idealized positions) are shown.

interactions involving other 5d metals.[6a,38] Due to the presence of two ^{t}Bu groups on each phosphine, it is possible to have an "internal standard" to accurately gauge the magnitude of bond deformation inherent in the agostic interactions. For example, in the cation shown in Figure 3, the Ir(63)−P(64)−C(^{t}Bu) angle of the agostic ^{t}Bu group is 20.5° less than the noninteracting ^{t}Bu group of the same phosphine. The six agostic (96.7−98.4°)/nonagostic (114.3−117.3°) ^{t}Bu groups in the three cations give an average Ir−P−C angle decrease of 18.6°.

Since the two agostic interactions are mutually cis, the hydrides must be cis also. In an effort to understand whether the cis orientation of the hydride ligands is a result of the agostic interactions from phosphine C−H bonds, the structure of $Ir(H)_2(PH_3)_2^+$ was optimized at the B3LYP level with no symmetry constraint.[39a] Despite the lack of steric hindrance or Ir−agostic interactions from PH_3 ligands, the optimized geometry shows a preference for trans phosphines and a cis arrangement for the hydrides (to minimize mutual influence of trans hydrides).[39b] The calculated H−Ir−H angle of 88.2° in the absence of agostic interactions shows that the cis hydride orientation in the experimental structure is consistent with a minimum-energy conformation in the absence of, and not caused by, the cis agostic interactions. The bent "saw-horse" ML_4 structure (essentially an octahedron with two cis ligands missing) of d^6 Ir(III) is more stable than square-planar or tetrahedral since it is the only geometry associated simultaneously with three nonbonding occupied d orbitals and two strong M−H interactions.The LUMO is the out-of-phase combination of a metal d orbital (*xy*) and the hydride orbitals. Because of the strong overlap and of the electropositive character of hydride, the LUMO is at high energy, leading to a large HOMO−LUMO gap (larger than in a tetrahedron or a square-pyramid structure).

Synthesis and Characterization of $[IrH(\eta^2\text{-}C_6H_4P^tBu_2)(P^tBu_2Ph)][BAr'_4]$. Ortho-metalation of a phenyl group on a phosphine ligand is a common reaction for low-valent unsaturated metal complexes, and is promoted by the presence of large (i.e., ^{t}Bu) pendant groups on the phosphine,[8] in contrast to the rarity of ortho-metalation involving PMe_2Ph.[40] The metalation of a phosphine can have a profound influence on the reactivity of the complex and radically change the steric profile of the phosphine ligand. The effective cone angle of the metalated phosphine increases and can promote the dissociation of other ligands via increased steric repulsions (i.e., labilizing effect).[21]

The addition of 1 equiv of $Na[BAr'_4]$ to $IrH(\eta^2\text{-}C_6H_4P^tBu_2)(Cl)(P^tBu_2Ph)$ in CH_2Cl_2 leads to a rapid abstraction of the chloride ligand and formation of $[IrH(\eta^2\text{-}C_6H_4P^tBu_2)(P^tBu_2Ph)][BAr'_4]$. This complex can be isolated as an orange

(33) For comparison, see: Wasserman, H. J.; Kubas, G. J.; Ryan, R. R. *J. Am. Chem. Soc.* **1986**, *108*, 2294.

(34) Strauss, S. H. *Chem. Rev.* **1993**, *93*, 927.

(35) For a discussion of this concept in the structural analysis of inorganic complexes, see: Martin, A.; Orpen, A. G. *J. Am. Chem. Soc.* **1996**, *118*, 1464.

(36) For an example of a bis-agostic interaction, involving two phenyls, to a single coordination site, see: King, W. A.; Luo, X.-L.; Scott, B. L.; Kubas, G. J.; Zilm, K. W. *J. Am. Chem. Soc.* **1996**, *118*, 6782.

(37) (a) Crabtree, R. H.; Holt, E. M.; Lavin, M.; Morehouse, S. M. *Inorg. Chem.* **1985**, *24*, 1986. (b) Robertson, G. B.; Wickramasinghe, W. A. *Acta Crystallogr., Sect. C: Cryst. Struct. Commun.* **1988**, *44*, 1383.

(38) Crabtree, R. H. *Chem. Rev.* **1985**, *85*, 245.

(39) (a) Cooper, A. C.; Streib, W. E.; Eisenstein, O.; Caulton, K. C. *J. Am. Chem. Soc.* **1997**, *119*, 9069. (b) For relevant theoretical precedent, see: Burdett, J. K. *J. Chem. Soc., Faraday Trans. 2* **1974**, *70*, 1599. Elian, M.; Hoffmann, R. *Inorg. Chem.* **1975**, *14*, 1058.

(40) Green, M. A.; Huffman, J. C.; Caulton, K. G.; Rybak, W. K.; Ziolkowski, J. *J. Organomet. Chem.* **1981**, *218*, C39.

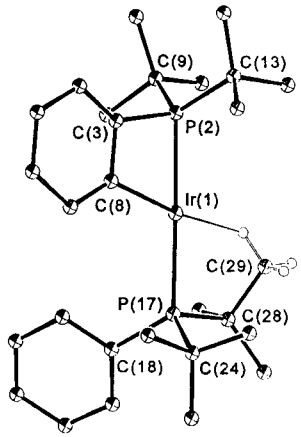

Figure 4. ORTEP drawing of IrH(η^2-$C_6H_4P^tBu_2$)(P^tBu_2Ph)$^+$ showing selected atom labeling. Only the hydrogens of the agostic methyl groups (placed in idealized positions) are shown.

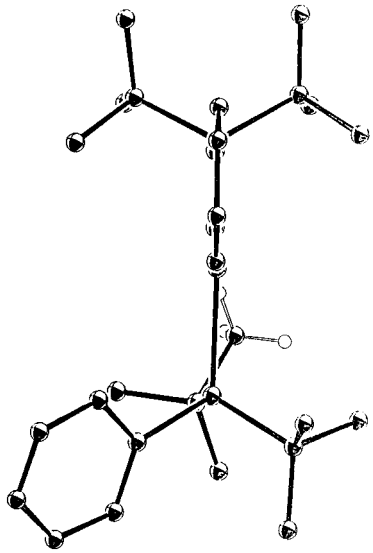

Figure 5. Edge-on view of the Ir−C−P−P plane of IrH(η^2-C_6H_4P-$^tBu_2$)(P^tBu_2Ph)$^+$.

crystalline material by recrystallization from benzene. The ^{1}H and ^{31}P{^{1}H} NMR spectra of the product confirms that the ortho-metalation present in the starting material is retained after chloride abstraction. ^{1}H NMR shows four doublets for inequivalent ^{t}Bu groups and a doublet of doublets in the upfield region for the hydride ligand, due to coupling of the hydride to two inequivalent phosphorus nuclei. ^{31}P{^{1}H} NMR shows an AX pattern for the two phosphines, with a large coupling constant of 278 Hz, characteristic of a mutually trans configuration. Variable-temperature NMR studies in CD_2Cl_2 are not able to show any features consistent with agostic bonding by either ^{t}Bu or phenyl groups. However, the crystal structure of [IrH(η^2-$C_6H_4P^tBu_2$)(P^tBu_2Ph)][BAr′$_4$] (Figures4 and 5) shows a strong agostic interaction from a ^{t}Bu group of the terminal phosphine ligand.

Despite the presence of two empty coordination sites, only one agostic interaction is observed. The anion is noncoordinating, and no solvent ligands are present. Examination of the structural data (Table 5) shows the extreme deformations of the metalated phosphine that are necessary to form the covalent Ir−C bond. The P−Ir−P angle (177.58°) is very close to 180°, showing that the cyclometalation does not significantly affect the trans coordination of the phosphines. The bond angle contractions needed to form the strained four-membered metallacycle occur at the Ir−P−C(ipso) and P−C(ipso)−C(ortho) angles of the ring. The Ir−P−C(ipso) and P−C(ipso)−C(ortho) angles (83.9° and 101.5°) are 35.0° and 19.5° smaller than the corresponding angles of the nonmetalated phosphine. The agostic interaction (trans to metalated phenyl) is characterized by a short Ir−C distance (2.745 Å, 0.06−0.19 Å shorter than agostic Ir−C in [Ir(H)$_2$(P^tBu_2Ph)$_2$][BAr′$_4$]) and a contraction of the Ir−P−C angle involving the agostic ^{t}Bu group (94.2°, 2.5−4.2° smaller than the agostic Ir−P−C in [Ir(H)$_2$(P^tBu_2Ph)$_2$][BAr′$_4$]). By these criteria, this agostic interaction is stronger than those observed for [Ir(H)$_2$(P^tBu_2Ph)$_2$][BAr′$_4$]. The hydride ligand and phosphine hydrogens of [IrH(η^2-$C_6H_4P^tBu_2$)(P^tBu_2-Ph)][BAr′$_4$] were not located by the X-ray diffraction. Placing the hydrogens of the agostic methyl group in idealized positions and setting the C−H bond distance at 1.05 Å results in a short (2.032 Å) Ir−H distance. These restrict the ability of the ^{t}Bu groups of the metalated phosphine to reach the empty coordination site, which might have furnished another agostic interaction.

Table 5. Selected Bond Distances (Å) and Angles (deg) for [IrH(η^2-$C_6H_4P^tBu_2$)(P^tBu_2Ph)][BAr′$_4$]

Ir(1)−C(29)	2.745(9)	Ir(1)−P(2)	2.319(3)
Ir(1)−C(8)	2.042(9)	Ir(1)−P(17)	2.333(3)
P(2)−Ir(1)−P(17)	177.58(13)	Ir(1)−P(17)−C(28)	94.2(4)
P(2)−Ir(1)−C(8)	68.7(3)	Ir(1)−P(17)−C(24)	116.9(4)
P(2)−C(3)−C(8)	101.5(7)	Ir(1)−P(2)−C(9)	115.82(10)
Ir(1)−P(2)−C(3)	83.9(3)	Ir(1)−P(2)−C(13)	117.17(10)
P(17)−Ir(1)−C(8)	111.2(3)	P(17)−C(28)−C(29)	104.0(7)
Ir(1)−P(17)−C(18)	118.9(4)		

To form an agostic interaction from a ^{t}Bu group of the metalated phosphine, two of the Ir−P−C angles would have to be less than 100°. The resulting geometry about the phosphorus atom would be significantly distorted from tetrahedral and should be very high in energy. The failure of the second ^{t}Bu group of the already agostic phosphine ligand (i.e., P(17)) to form another agostic interaction, giving two agostic interactions from one phosphine, can be attributed to the same effect. Thus, the geometrical constraints imposed by ortho-metalation and the agostic interaction trans to phenyl prevent agostic bonding to the empty coordination site despite the presence of three pendant ^{t}Bu groups.

Synthesis and Characterization of [Ir(H)$_2$(PCy_2Ph)$_3$][BAr′$_4$]. An analogue of [Ir(H)$_2$(P^tBu_2Ph)$_2$][BAr′$_4$], incorporating smaller alkyl groups on the phosphines, was desired to probe for the effect of these groups on the formation (or lack) of agostic interactions. Attempts at the synthesis of [Ir(H)$_2$(PCy_2-Ph)$_2$][BAr′$_4$] were unsuccessful. Abstraction of the chloride ligand from Ir(H)$_2$Cl(PCy_2Ph)$_2$ by Na[BAr′$_4$] gave a mixture of products including [Ir(H)$_2$(PCy_2Ph)$_3$][BAr′$_4$] and monophosphine hydride complexes (characterized by doublet splitting of the hydrides in the ^{1}H NMR spectrum). [Ir(H)$_2$(PCy_2Ph)$_3$][BAr′$_4$] could be isolated in low yield from these mixtures by crystallization from hot benzene. The following rational synthesis of [Ir(H)$_2$(PCy_2Ph)$_3$][BAr′$_4$] was therefore devised: the addition of 1 equiv of Na[BAr′$_4$] to "Ir(H)$_2$Cl(PCy_2Ph)$_3$" (generated in situ from [Ir(COE)$_2$Cl]$_2$, 6 equiv of PCy_2Ph, and excess H_2) in CH_2Cl_2 or fluorobenzene results in the formation of [Ir(H)$_2$-(PCy_2Ph)$_3$][BAr′$_4$] in high yield. This formally 16-electron complex can be isolated as a crystalline solid, free of solvent ligands, by recrystallization from hot benzene.

The ^{1}H NMR spectrum of [Ir(H)$_2$(PCy_2Ph)$_3$][BAr′$_4$] in d_8-THF shows resonances in the phenyl region for the BAr′$_4$ anion and phenyl groups of the phosphines. A number of broad, overlapping resonances from 2.41 to 0.85 ppm are assigned to cyclohexyl protons. The hydride ligands are observed as a single

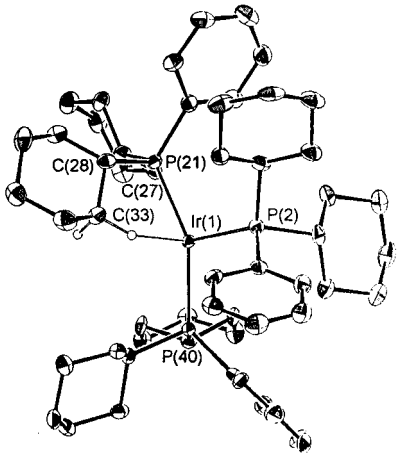

Figure 6. ORTEP drawing of $Ir(H)_2(PCy_2Ph)_3^+$, showing selected atom labeling. Only the hydrogens of the agostic methylene groups (placed in idealized positions) are shown.

broad resonance (singlet, −26.1 ppm) at room temperature, suggestive of a rapid site exchange between the hydride ligands.[41] Lowering the temperature results in a broadening of the hydride resonance and eventual decoalescence of two hydride signals at ca. −80 °C. At −110 °C, the ^{1}H NMR spectrum shows signals at −5.4 ppm (br doublet, $J_{PH} = 107$ Hz) and −44.8 ppm (br s, $w_{1/2} = 70$ Hz). These signals suggest a static structure (**I**) at this temperature, in which one hydride

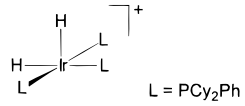

I

is trans to a phosphine, the other hydride is trans to the empty coordination site, and phosphines adopt a mer arrangement in a square pyramid. There are no significant changes in the phenyl or cyclohexyl resonances in the temperature range +25 to −110 °C.

Another fluxional process is observed in the variable-temperature $^{31}P\{^1H\}$ NMR spectra. At 25 °C, the three phosphines are observed as a single resonance at 28.3 ppm. Cooling the solution causes a broadening of this signal and decoalescence is observed at ca. −20 °C. At temperatures below −30 °C, two resonances are present at 28.9 and 28.2 ppm in a 2:1 integrated ratio. These data are consistent with a decoalescence of two phosphine environments in either a mer or fac $IrH_2P_3^+$ structure. Upon the basis of the strong trans influence of the hydrides, the mer configuration (**I**) should be favored. These signals remain broad down to −100 °C, and no phosphorus−phosphorus coupling is observed.

Unlike $[Ir(H)_2(P^tBu_2Ph)_2][BAr'_4]$, $[Ir(H)_2(PCy_2Ph)_3][BAr'_4]$ has very poor solubility in arene solvents. This unfortunate solubility problem has curtailed the study of a possible agostic interaction by NMR or IR spectroscopy in noncoordinating solvents. Therefore, the determination of the structure of $[Ir(H)_2(PCy_2Ph)_3][BAr'_4]$ by X-ray diffraction was performed (Figure 6).

Structural analysis of the IrP_3 unit (Table 6) shows a highly distorted mer arrangement for the phosphine ligands, due to the steric interactions inherent in the coordination of three bulky PCy_2Ph to the Ir. The axial phosphines are bent away from the equatorial phosphine, giving cis $P_{ax}-Ir-P_{eq}$ angles (103.95° and 106.09°) much greater than 90° and a trans P−Ir−P angle of the axial phosphines (149.95°), greatly reduced from 180°. The most interesting feature of the crystal structure of $[Ir(H)_2(PCy_2Ph)_3][BAr'_4]$ is an agostic interaction from a C−H bond of one of the cyclohexyl groups on an axial phosphine ligand. As expected, the BAr'_4 anion is noncoordinating, and crystallization from C_6H_6 resulted in no solvent coordination to the empty site. While the hydride ligands and hydrogens of the phosphines were not located in the X-ray study, the agostic interaction can be characterized by a number of structural parameters presented in Table 6.

Table 6. Selected Bond Distances (Å) and Angles (deg) for $[Ir(H)_2(PCy_2Ph)_3][BAr'_4]$

Ir(1)−P(2)	2.4005(16)	Ir(1)−P(40)	2.3587(16)
Ir(1)−P(21)	2.3163(17)	Ir(1)−C(33)	2.923(10)
P(2)−Ir(1)−P(21)	103.95(6)	C(33)−Ir(1)−P(2)	108.33(4)
P(2)−Ir(1)−P(40)	106.09(6)	Ir(1)−P(21)−C(28)	100.94(21)
P(21)−Ir(1)−P(40)	149.95(6)	Ir(1)−P(21)−C(22)	113.86(21)
C(33)−Ir(1)−P(40)	108.29(4)	P(21)−C(28)−C(33)	107.1(4)
C(33)−Ir(1)−P(21)	61.44(6)	P(21)−C(22)−C(27)	115.8(4)

The Ir−C distance (2.923 Å) to the agostic C−H is within the range of distances observed for the agostic Ir−C distances in $[Ir(H)_2(P^tBu_2Ph)_2][BAr'_4]$ (2.81−2.94 Å), implying that the strength of the interactions may be similar. The Ir−P−C(α) and P−C(α)−C(β) angles (100.94° and 107.1°) involving the agostic cyclohexyl group are significantly decreased from the corresponding angles of the pendant cyclohexyl of the same phosphine (113.86° and 115.8°).

Five-membered rings may be formed by agostic interaction with either a C−H bond of a cyclohexyl group or an *o*-phenyl C−H bond, but a preference to form the agostic interaction with the aliphatic group is demonstrated by the results presented here, as it also is in $[Ir(H)_2(P^tBu_2Ph)_2][BAr'_4]$ and $[IrH(\eta^2\text{-}C_6H_4P\text{-}^tBu_2)(P^tBu_2Ph)][BAr'_4]$. While the smaller cone angle of PCy_2Ph (estimated at 162°),[42] compared to P^tBu_2Ph, is apparent by the coordination of three phosphines in $[Ir(H)_2(PCy_2Ph)_3][BAr'_4]$, the steric bulk of the cyclohexyl and phenyl groups of the phosphine is still sufficient to promote an agostic interaction in $[Ir(H)_2(PCy_2Ph)_3][BAr'_4]$. Inter-phosphine repulsions are clearly apparent in the structure by the large deformations from a rigorous mer geometry (i.e., P−Ir−P bond angles of 90 and 180°). Therefore, both substituent effects from the pendant groups of the agostic phosphine *and* inter-phosphine steric repulsions must be considered in this case. This makes the consideration of the influence of steric factors on the agostic interaction more complicated than in the case of $[Ir(H)_2(P^tBu_2Ph)_2][BAr'_4]$, where the steric repulsions between mutually trans phosphines (P−Ir−P angle close to 180°) could be discounted.

Synthesis and Characterization of $[Ir(H)_2(P^iPr_2Ph)_3][BAr'_4]$. The synthesis and characterization of $[Ir(H)_2(P^iPr_2Ph)_3][BAr'_4]$ were accomplished in an effort to study the effect of changing the bulky substituents of the phosphine ligands from those in $[Ir(H)_2(PCy_2Ph)_3][BAr'_4]$ while minimizing the difference in phosphine donating ability. PCy_2Ph and P^iPr_2Ph should have very similar donating abilities, both containing P−C bonds to two secondary alkyls and one phenyl substituent.

The addition of 1 equiv of $Na[BAr'_4]$ to "$Ir(H)_2Cl(P^iPr_2Ph)_3$" (generated in situ from $[Ir(COE)_2Cl]_2$, 6 equiv of P^iPr_2Ph, and excess H_2) in CH_2Cl_2 or fluorobenzene results in the formation of $[Ir(H)_2(P^iPr_2Ph)_3][BAr'_4]$ in high yield. This formally 16-electron complex can be isolated as a crystalline solid, free of solvent ligands, by recrystallization from benzene.

(41) Gusev, D. G.; Berke, H. *Chem. Ber.* **1996**, *129*, 1143.

(42) Tolman, C. A. *Chem. Rev.* **1977**, *77*, 313.

Table 7. Selected Bond Distances (Å) and Angles (deg) for $[Ir(H)_2(P^iPr_2Ph)_3][BAr'_4]$

Ir(1)−P(2)	2.323(6)	Ir(1)−P(28)	2.320(10)
Ir(1)−P(15)	2.394(8)	Ir(1)−C(37)	3.463(8)
P(2)−Ir(1)−P(28)	146.4(3)	Ir(1)−P(28)−C(29)	126.7(10)
P(2)−Ir(1)−P(15)	107.79(24)	Ir(1)−P(28)−C(35)	108.5(14)
P(15)−Ir(1)−P(28)	105.8(3)	Ir(1)−P(28)−C(38)	110.4(13)
Ir(1)−P(2)−C(3)	122.5(10)	Ir(1)−P(2)−C(12)	108.3(9)
Ir(1)−P(2)−C(9)	114.2(9)		

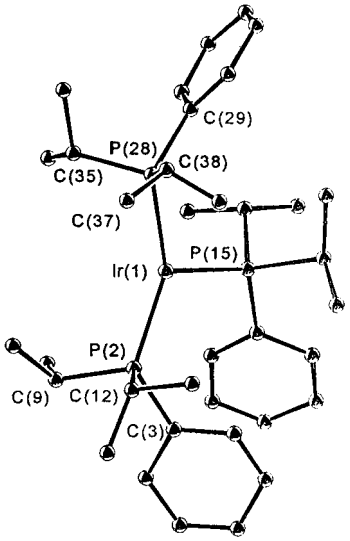

Figure 7. ORTEP drawing of $Ir(H)_2(P^iPr_2Ph)_3^+$, showing selected atom labeling.

Variable-temperature ^1H and $^{31}P\{^1H\}$ NMR spectra of $[Ir(H)_2(P^iPr_2Ph)_3][BAr'_4]$ in d_8-THF are very similar to those observed for $[Ir(H)_2(PCy_2Ph)_3][BAr'_4]$. The room-temperature ^1H NMR spectra show the expected resonances for the BAr'_4 and P^iPr_2Ph protons. The hydride ligands are observed at 25 °C as a single broad resonance at −25.4 ppm. Cooling the solution to ca. −80 °C causes decoalescence of the two hydrides as separate, broad signals at −5.8 and −43.8 ppm. Large P−H coupling (104 Hz) can be resolved on the downfield hydride signal at −100 °C. The $^{31}P\{^1H\}$ NMR spectrum at room temperature shows one resonance at 35.2 ppm, which decoalesces into two signals at 35.4 and 34.4 ppm (2:1 integrated ratio) at ca. −30 °C. Due to the large line width of these signals, no phosphorus−phosphorus coupling is observed at any temperature down to −100 °C.

The structure of $[Ir(H)_2(P^iPr_2Ph)_3][BAr'_4]$ was determined by X-ray diffraction. While the angles of the IrP_3 core (Table 7) show a distorted mer geometry in which the trans phosphine ligands are distorted away from the equatorial phosphine ligand (Figure 7), closely resembling those of $[Ir(H)_2(PCy_2Ph)_3][BAr'_4]$, there is a notable lack of any agostic bond to the empty coordination site in $[Ir(H)_2(P^iPr_2Ph)_3][BAr'_4]$. The shortest Ir−C distance is 3.338 Å, involving a methine carbon on an axial phosphine, and the shortest Ir−C(methyl) distance is 3.463 Å, clearly inconsistent with Ir···H−C bonding. There is no perceptible contraction of any Ir−P−C angles, further proving the lack of any agostic interaction in $[Ir(H)_2(P^iPr_2Ph)_3][BAr'_4]$. The ^{i}Pr and Cy analogues are thus *not* isostructural! Indeed, the crystals are not even isomorphous.

Comparison of $Ir(H)_2P_3^+$ Structures. The geometrical distortions necessary to form the five-membered ring of an agostic bond in $[Ir(H)_2(PCy_2Ph)_3][BAr'_4]$ become apparent when this structure is compared directly to that of $[Ir(H)_2(P^iPr_2Ph)_3][BAr'_4]$ (Figure 8). The contracted Ir−P−C angle of the agostic cyclohexyl group in $[Ir(H)_2(PCy_2Ph)_3][BAr'_4]$ is clearly not present in $[Ir(H)_2(P^iPr_2Ph)_3][BAr'_4]$. Note that the configurations of alkyl and phenyl groups in the phosphine ligands of the two structures are nearly identical, suggesting that the effect of intermolecular contacts within the crystal on the configuration of the phosphine substituents is minimal. These conformations must be determined primarily by intramolecular contacts.

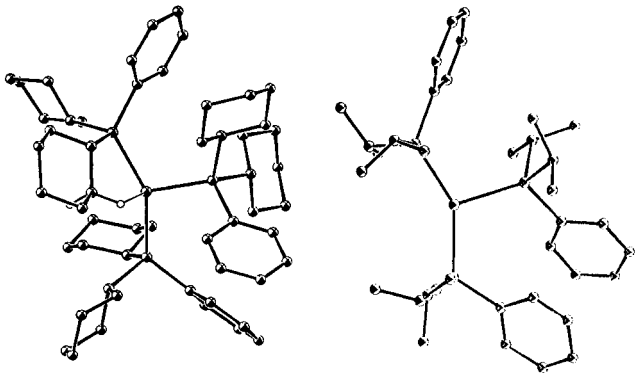

Figure 8. ORTEP drawings of $Ir(H)_2(PCy_2Ph)_3^+$ (left) and $Ir(H)_2(P^iPr_2Ph)_3^+$ (right) viewed to show the similarity of the phosphine substituent conformations. Only the agostic methylene group hydrogens are shown at left.

If so many similarities between the two structures exist, how then can one contain an agostic interaction, while the other does not? Differences in the electrophilicity of the Ir centers should be minimal. The donating ability of the two phosphines is expected to be very similar, and the first coordination spheres are nearly identical. Thus, it is reasonable to conclude that, in determining the formation (or lack) of agostic bonds in these two complexes, steric effects predominate. The origin of the difference in the structures appears to lie mainly in the identity of the alkyl groups of the phosphine ligands. Cyclohexyl apparently has a larger steric impact than isopropyl, as evidenced by the difference in the cone angles of PCy_3 (170°) vs P^iPr_3 (160°).[42] Cyclohexyl ring constraints limit distortions of the β-methylene groups which might otherwise lower steric repulsions. The methyl groups of isopropyl have no such constraint. For the molecules $[Ir(H)_2(PR_2Ph)_3][BAr'_4]$, the average of the C−P−C angles of the nonagostic phosphines is (slightly) larger for R = Cy (103.2°) vs R = ^{i}Pr (102.4°). Larger C−P−C angles are characteristic of increased steric repulsions among the alkyl groups of the phosphine.

Calculational Evidence for the Importance of Substituent Bulk on Agostic Interactions. (a) Agostic Interaction: Electronic and/or Steric Origin? The hybrid (QM/MM) IMOMM method[16] has been successful in reproducing various types of distortion of the coordination sphere caused by bulky ligands.[17] In the particular case of unsaturated molecules, the attempt to decrease intraligand and interligand repulsive interactions can direct pendant groups toward the space left vacant by the missing ligand. In doing so, a C−H bond could come sufficiently close to the metal to be viewed as being involved in agostic interaction. A fundamental question thus arises: is the short M···H−C distance the result of minimizing steric repulsion with no additional attractive M−C−H attraction or is there also an attraction between the weak C−H Lewis base and the Lewis acid empty metal site? The theoretical studies presented in a previous communication on $Ir(H)_2(P^tBu_2Ph)_2^+$ have shown the determining influence of steric factors for bringing CH_3 within bonding distance of the metal.[15] When the real complex is modeled by $Ir(H)_2(PH_2C_2H_5)_2^+$, B3LYP calculations show the

Table 8. Experimental and Calculated Structural Parameters for $Ir(H)_2(PCy_2Ph)_3^+$, Using Various Computational Models (see Text)

	exptl	B3LYP/I	MP2/I	B3LYP/II	MP2/II
Ir−P(21)	2.316	2.381	2.374	2.375	2.350
Ir−P(40)	2.359	2.419	2.400	2.424	2.400
Ir−P(2)	2.400	2.528	2.508	2.529	2.500
P(21)−Ir−P(40)	150.0	152.6	152.0	152.0	151.0
P(2)−Ir−P(21)	104.0	102.0	102.3	102.9	103.0
P(2)−Ir−P(40)	106.0	105.4	105.6	105.0	105.9
Ir···C(33)	2.923	3.178	3.176	3.107	2.881
Ir−P(21)−C(28)	100.9	105.6	105.5	103.8	99.8
Ir−P(21)−C(27)	113.9	111.0	111.4	110.4	111.6
av angle at P(3)	109.7	109.6	109.9	109.4	109.9

absence of agostic interaction since the C atom remains 3.98 Å from the metal. The calculated ∠Ir−P−C_α is 118.8°, compared to the experimental value of 97°. The energy gain associated with the weak C−H···Ir interaction is thus too small to effect the necessary bending of the Ir−P−C angle. While $IrH_2L_2^+$ is a 14-electron and thus highly electron-deficient complex, the two hydrides with their strong trans influence limit the energy gain of bonds trans to the hydrides.

The IMOMM calculations on this same $Ir(H)_2(P^tBu_2Ph)_2^+$ complex were carried out with $Ir(H)_2(PH_2C_2H_5)_2^+$ in the QM part. The results mimic well the Thorpe−Ingold effect mentioned earlier.[14] Remarkably, this is achieved primarily by decreasing the Ir−P−C_α angle (102.6°) and leaving the P−C_α−C_β angles essentially undistorted. While the calculations clearly illustrate the importance of the full ligand in achieving agostic interactions, they do not permit separation of the electronic and steric components in the agostic interaction. The carbon chain carrying the agostic group is part of the QM ensemble, while the other substituents at the phosphorus are part of the MM ensemble. We extend here the previous study to the $Ir(H)_2(PCy_2Ph)_3^+$ and $Ir(H)_2(P^iPr_2Ph)_3^+$ species containing three phosphine groups, and we propose also a way to have a better understanding of the true factors by doing two sets of calculations with different partitioning of the substituents of the phosphine ligands in the QM and MM ensembles.

(b) $Ir(H)_2(PCy_2Ph)_3^+$. The complex $Ir(H)_2(PCy_2Ph)_3^+$ was calculated by the IMOMM method. Two sets of partitioning of atoms between the QM and MM domains have been chosen. In model I, all atoms that are not directly bonded to the metal are calculated at the MM level. This means that for the QM part, the phosphine is represented by PH_3 and that the C−H bonds in the vicinity of the metal carry *no* electronic density. In model II, the QM part of the phosphine includes $PH_2C_2H_5$, where the terminal C−H bond of the ethyl substituent is that which could come into proximity to the metal center. The remaining part of this cyclohexyl as well as the second cyclohexyl and the phenyl group are part of the MM calculations. Model II differs from model I in that electron density is present in the C−H bond which could come into proximity to the metal center. Two levels of calculations, B3LYP and MP2, were selected for the QM part. While B3LYP has had large success for providing very good geometries in transition metal complexes, it underestimates weak interactions.[43] The MP2 method has also given good results for geometry and seems to give a better representation of weak interactions. Its wide use has been limited because of its requirement in computational effort.

$Ir(H)_2(PCy_2Ph)_3^+$ was fully optimized at four levels: B3LYP and MP2 for models I and II (B3LYP or MP2/I or II). The most relevant geometrical parameters from these four calculations are given in Table 8, along with the experimental values. Figure 9 shows the calculated structure resulting from MP2/II level and is qualitatively similar for all methods of calculations. Numbering of heavy atoms is identical to that in the experimental structure.

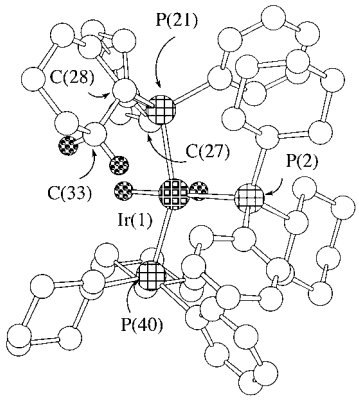

Figure 9. Optimized (MP2/MM3) structure of $Ir(H)_2(PCy_2Ph)_3^+$.

At all levels of calculations, the geometry is that of a strongly distorted square-based pyramid with one apical hydride. The overall coordination of the Ir atom is well reproduced, and the angles P−Ir−P differ from the experimental value by less than 2°. The P(21)−Ir−P(40) angle of 150° and the P(2)−Ir−P(21) and P(2)−Ir−P(40) angles of 105° clearly reflect the large bulk of the PCy_2Ph groups. The calculated Ir−P(21) and Ir−P(40) bond distances are longer than the experimental values by 0.065 Å, while the discrepancy is even larger (0.13 Å) for Ir−P(2), which is trans to a hydride. The best agreement is obtained for MP2/II. Models I and II give reasonably close results within the same method of quantum calculations. Using B3LYP in place of MP2 results in an increase in the calculated Ir−P bond lengths. It is, however, satisfying that all levels of calculations reproduce the relative Ir−P bond lengths.

From the X-ray results, the shortest Ir···C(33) distance (2.923 Å) indicates the presence of an agostic C−H bond. Associated with this short distance is a strong decrease in the Ir−P(21)−C(28) angle, to 100.9°, while the Ir−P(21)−C(27) (nonagostic cyclohexyl) angle is 113.9°. For the other phosphine ligands, the experimental Ir−P−C(cyclohexyl) angles are around 110°. For B3LYP/I and MP2/I calculations, the angles for the nonagostic groups are quantitatively reproduced within 0.5°. The trend in the angles at P(21) is correctly represented since the smallest value (105.5°) is for Ir−P(21)−C(28) (agostic cyclohexyl), while the Ir−P(21)−C(27) (nonagostic cyclohexyl) is 111.0°. Angles at the carbon centers are all around 109°. Thus, as for $IrH_2(P^tBu_2Ph)_2^+$, the essentials of the Thorpe−Ingold effect are visible in the distorted Ir−P−C angles. Since ∠Ir−P(21)−C(28) is slightly too large and since the Ir−P bonds are also too long, the calculations with model I (B3LYP or MP2) give an Ir···C(33), which is 0.25 Å too long (3.18 Å) and equal for the two quantum methods.

Since model I describes the cyclohexyl and phenyl group at the MM level only, the results of the calculations show that the bulk of the ligands alone, in the absence of any attractive forces between the metal and C−H bonds, has positioned one of the cyclohexyl substituents with one C−H bond in the vicinity of the empty site of the metal. However, the distance M···H is beyond any bonding interaction. The ability to determine the consequence of only one type of interaction (here, steric) is a strength of the hybrid method: the execution of "computational experiments".

(43) Ruiz, E.; Salahub, D. R.; Vela, A. *J. Phys. Chem.* **1996**, *100*, 12265.

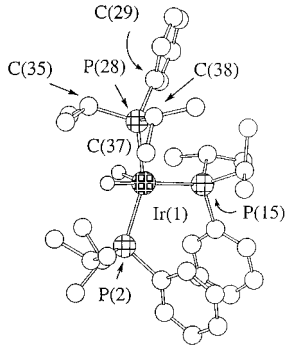

Figure 10. Optimized (MP2/MM3) structure of $Ir(H)_2(P^iPr_2Ph)_3^+$.

With model II, the Ir···C(33) distances are shorter than with model I and the best results are obtained for the MP2 calculations (Ir···C(33) = 2.881 Å, which is very close to the experimental value of 2.923 Å). For this calculation, there is excellent agreement for all Ir−P−C angles, including the one corresponding to the agostic cyclohexyl group. The B3LYP/II calculations give a significantly greater distance Ir···C(33) (3.107 Å). In fact, the distance Ir···C(33) is only slightly shorter than for the pure molecular mechanics model of cyclohexyl (method I). This confirms that the B3LYP significantly underestimates the energy of the electronic part of the agostic interaction.

The two factors that are important in this complex for the occurrence of the agostic interaction are clearly apparent in these calculations. The steric bulk of the ligands moves one cyclohexyl group into proximity of the metal empty site as shown by the pure molecular mechanics calculations (method I). It is remarkable that the orientation of all the ligands in the calculated structure is identical to that in the calculated structure. This shows that the structure adopted by the compound in the solid state is at least a local minimum on the potential energy surface for the isolated molecule and also suggests a very small influence of the crystal packing. When the level of calculations is changed from method I to method II, the conformations of the substituents of the phosphine remain identical. The only consequence of the model I/II upgrade is that the C−H bond moves toward the metal, showing the presence of a true attraction between Ir and the C−H bond. As expected, the agostic C−H bond is longer (1.11 Å) than those that are not in contact with the metal (1.09 Å) at the (MP2/II) level. The attraction of C−H toward the iridium center is accomplished primarily by bending the angle at the phosphine.

(c) $Ir(H)_2(P^iPr_2Ph)_3^+$. The complex $Ir(H)_2(P^iPr_2Ph)_3^+$ was calculated only with MP2/II, which maximizes the chance to locate an agostic interaction if it is present. Initiating the optimization process from the experimental geometry leads to a structure that is noticeably different from the experimental one (Figure 10). Several groups have rotated from the observed orientation in the solid state, and all of the Ir···C nonbonding distances are larger than 3.5 Å (3.4 Å experimentally). These facts are evidence for a shallow energy surface for the groups on the phosphine ligands, where orientation is not significantly influenced by any agostic interaction. The average of the ∠Ir−P−C(isopropyl) is calculated to be 115.7° (114.2° experimentally). The observed orientation of the ligands can then be influenced by the crystal packing.

Conclusions

The experimental structural comparison of $Ir(H)_2(PCy_2Ph)_3^+$ to $Ir(H)_2(P^iPr_2Ph)_3^+$ and the computational experiments on $Ir(H)_2(PR_2Ph)_n^+$, where R = ^{t}Bu, ^{i}Pr, and Cy, and simplified systems represent the "most pure" tests of the effect of steric constraints on agostic bonding. Both these experimental and theoretical studies seek to manipulate steric parameters within a system while bringing minimal changes to the electronic (bonding) parameters (i.e., electron density of metal orbitals). Such careful changes are necessary when studying a phenomenon which relies on *both* steric and electronic factors. Based upon these studies, the lowering of the energetic barriers of bond deformation and loss of rotational entropy by bulky substituents on the agostic ligand, placing the C−H in the proximity of the empty coordination site, play *the* critical role in the formation of agostic bonds to these unsaturated iridium complexes.

The agostic bond is clearly very weak in these systems, probably because of the presence of the two hydrides. This permits the steric factors to play an active ("encouraging" or supporting) role in making the agostic interactions feasible. It also permits the agostic interaction to be remarkably sensitive to small changes in the nature of the phosphine. In this work, the subtle change between the two secondary alkyls ^{i}Pr and cyclohexyl is enough to cause an agostic interaction to be absent/present. Of course, steric factors are not mandatory for agostic interactions, as evidenced by the numerous examples deprived of any apparent steric strain.[44] Finally, the hybrid QM/MM method is a powerful tool for detecting and analyzing the relative role of the electronic and steric factors.

Acknowledgment. This work was supported by the U.S. National Science Foundation, the University of Montpellier, and the French CNRS. F.M. thanks the French CNRS for a position of research associate.

Supporting Information Available: Tables giving full crystallographic details, positional and thermal parameters, and bond distances and angles (23 pages, print/PDF). See any current masthead page for ordering information and Web access instructions.

JA981727E

(44) For recent references, see inter alia: (a) Han, Y. Z.; Deng, L. Q.; Ziegler, T. *J. Am. Chem. Soc.* **1997**, *119*, 5939. (b) Deng, L. Q.; Margl, P.; Ziegler, T. *J. Am. Chem. Soc.* **1997**, *119*, 1094. (c) Musaev, D. G.; Froese, R. D. J.; Svensson, M.; Morokuma, K. *J. Am. Chem. Soc.* **1997**, *119*, 367. (d) Musaev, D. G.; Svensson, M.; Morokuma, K.; Stromberg, S.; Zetterberg, K.; Siegbahn, P. E. H. *Organometallics* **1997**, *16*, 1933. (e) Woo, T. K.; Fan, L.; Ziegler, T. *Organometallics* **1994**, *13*, 2252.